Presented at the Symposium on Modern
Developments in HSLA Formable Steels,
Chicago, IL, October 20, 1977

LBL-6995

c.2

DESIGN OF DUPLEX LOW CARBON STEELS FOR IMPROVED STRENGTH: WEIGHT APPLICATIONS

J. Y. Koo and G. Thomas

March 1978

Prepared for the U. S. Department of Energy
under Contract W-7405-ENG-48

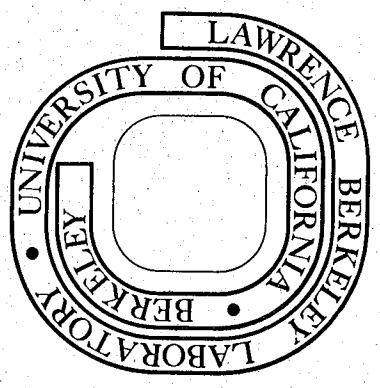

LBL-6995

c.2

DISCLAIMER

Paper to the symposium proceeding, "Modern developments in HSLA Formable Steels". Edited by A. T. Davenport.

DESIGN OF DUPLEX LOW CARBON STEELS FOR IMPROVED STRENGTH: WEIGHT APPLICATIONS

J. Y. Koo and G. Thomas

Materials and Molecular Research Division
Lawrence Berkeley Laboratory
and
Department of Materials Science and Mineral Engineering
University of California
Berkeley, California 94720

ABSTRACT

Design principles for improved mechanical properties of Duplex Ferrite-Martensite (DFM) steels have been evaluated in order to obtain desirable microstructural characteristics which in turn result in desirable mechanical properties. A DFM alloy, of composition Fe/2% Si/0.1% C, has been developed according to the design criteria. This 2% Si DFM steel showed high strength and good formability, and its tensile properties are superior to a series of Cr and Mn containing DFM steels, and to some selective commercial HSLA steels including Van 80. Over the range of 15 $\sim$ 80% martensite the "composite" rule for two phase mixtures appears to hold as a fairly good approximation of the tensile behavior of the duplex systems investigated.

The effect of the property variations of the individual constituents, and duplex structure-property relations are also presented.

INTRODUCTION

During the past several years, the duplex ferrite-martensite (DFM) steels have received increasing emphasis, especially in the transportation industries, due to the characteristic microstructural features which combine high strength with good formability. The strengthening principle of the DFM structure involves the incorporation of inherently strong martensite as a load carrying constituent in a soft ferrite matrix. The latter supplies the system with the essential ductility.

Apart from these interesting mechanical properties, however, there is a general lack of fundamental understanding of the characteristic behavior of DFM steels. For instance, papers reporting the results of mechanical property tests generally made little direct correlations with duplex microstructures, except for some occasional optical metallography.[1-3] The mechanical behavior of the two phase materials as well as the intricate interactions of parameters such as the size, shape, distribution, and volume fraction of martensite particles, must all be characterized and controlled in designing improved DFM alloys such that they favorably contribute in concert to the overall mechanical properties.

In the present paper, the principles of our current alloy design program, which has been adopted to achieve optimum balances of strength and ductility, are briefly described.

Principles Of DFM Alloy Design Program

The main principles of the alloy development can be summarized as follows:

1. Obtain the (α+ martensite) duplex structures by phase transformation alone.
2. Control the % C in martensite to $\sim$0.3% to avoid twinned martensite.
3. Alloys must have a large slope in the A_3 line.
4. Optimize the properties of the constituent phases.

DFM structures can be produced in many different ways[4], as has been demonstrated over the last 40 years.[5-9] We restrict the present approach to employ only simple heat treatment by annealing in the two-phase ($\alpha+\gamma$) field and quenching without resorting to mechanical or thermo-mechanical treatments. The initial alloy composition and volume pct. martensite are properly controlled so that the carbon concentration in the martensite phase is approximately 0.3 wt.%. As a result, during martensitic transformation the inhomogeneous shear component occurs by slip, not twinning.[10] Hence, unlike many other composite systems in which the second phases are in most cases strong and brittle, the property of the martensite constituent will be both strong and tough, as has been shown in our parallel alloy design program on structural martensitic steels.[10] Thus the results of this latter program have been helpful in the development of the duplex alloy steel program.

From a practical point of view, it is desirable to have a large slope in the A_3 line in order to have flexibility in heat-treatment for control of volume fraction of the two phases. This can be achieved

by adding suitable ternary alloying elements (e.g., Si)[11] to the Fe-C base system, as is illustrated in Fig. 1. In Fig. 1a any slight variation in the two phase annealing temperature will shift composition as well as volume fraction of austenite (and hence martensite) to a great extent, whereas in the case of Fig. 1b less stringent control on the critical annealing temperature is required, thereby increasing the flexibility for heat treatment.

It is also important to take into account the parameters such as optimum volume fraction of martensite (V_m), distribution of martensite particles, and minor constituents, e.g., carbides and retained austenite. Qualitatively, the lower limit of the acceptable range of V_m is restricted to the value where no strengthening of the duplex alloy occurs. The upper limit is set when the failure of the martensite immediately leads to the failure of the duplex structure. Of course the final range of V_m will be determined by particular specifications and applications for which the steel will be used. The system is obviously rather flexible.

In adding second phase particles to ductile matrices, ductility is usually sacrificed for strength. However, one can imagine from the many possible duplex distributions of martensite particles, a suitable morphology which should provide not only strengthening but also a minimal loss in ductility. In this regard, a fine scale, discontinuous, and fibrous distribution of martensite particles are considered to be desirable.[4]

The composition of the DFM steels under consideration is based primarily on low carbon and low alloy. The resultant lack of sufficient

hardenability may cause the ferrite-carbide (eutectoid) transformation products to be formed during cooling from austenite to martensite. These carbides, if any, will be located only in the immediate vicinity of the α/martensite interfaces, and therefore should be avoided.[12] This can be accomplished only by quenching fast enough or by adding the proper alloying elements to suppress carbide formation.

The most difficult challenge is to produce DFM steels with these design considerations at a sufficiently small cost to make them economically competitive. We start with simple ternary Fe/X/C alloys prior to advancing to a more complex system.[4] Metallurgical knowledge accumulated to date on the behavior of alloying elements (x) suggest that silicon is one of those which most favorably controls the design parameters of interest here.[13] In addition, silicon provides very effective solid solution strengthening in the ferrite.

Experimental

The compositions of the alloys investigated are listed in Table 1. High purity 1010 and 1020 alloys were vacuum melted and cast as 20 lb ingots. These ingots were subsequently upset forged to approximately 0.5 in. thickness. Portions were further reduced to approximately 0.15 in. by cold rolling. The experimental Fe/X/0.1 C alloys were prepared and provided by Daido Steel Co. Japan. The alloys were melted in a vacuum induction furnace. The ingots were then forged in the range 1000--1100°C into 15 mm diameter rods. They were homogenized at 1200°C in vacuum for 20 hrs and subsequently furnace-cooled. The heat treatment to produce controlled DFM structures consisted of austenitizing and

quenching to 100% martensite, followed by annealing in the (α+γ) range (details are described elsewhere[13]).

Tempering, when employed, was accomplished by the immersion of samples in a neutral salt bath kept at desired temperatures (200°C). All specimens were directly water quenched from the tempering temperature. Tensile properties were determined using 1 inch gage round tensile specimens, following ASTM specifications. Two inch gage round specimens were also used only when comparisons with the tensile properties of commercial steels were made. Tensile tests were performed at room temperature in an Instron machine with a cross-head speed of 0.05 cm/min and a full scale load of 1000 Kg.

The experimental procedures for optical metallography and transmission electron microscopy are given elsewhere.[4]

RESULTS AND DISCUSSION

DFM Structures Observed In Si Containing Steels:

Figure 2 shows an optical micrograph of the fibrous DFM structures developed in Si containing steels, as a result of the dual phase annealing and quench treatment. A magnified view of the individual martensite particles is shown in the transmission electron micrograph (Fig. 3), obtained from the 2% Si DFM steel. As the Si content was lowered, the major structural features remain unchanged but brittle carbides were present near the α/martensite interfaces. This is illustrated in Fig. 4 taken from 0.5% Si DFM steel. This morphology of carbide distribution is very similar to that of the interphase precipitation transformation product observed in a variety of steels.[14-15]

Nature Of α/Martensite Interface:

Since the load bearing constituent is the martensite phase, the nature of the α-martensite interface (coherent or not) is of particular importance. Fig. 5 shows the conventional bright field (a) and corresponding high resolution lattice fringe image (b) of an α/martensite interface in the 2% Si DFM steel. As the (110) fringes cross the interface, they are distorted but are continuous except for occasional end-on dislocations. The continuity in this case is interpreted as follows. Assuming the K-S orientation relationship holds in the $\alpha + \gamma$ mixture at 950°C then for $(111)_\gamma$ the particular variant of the six possible $\{110\}_\alpha$ will be the $(101)_\alpha$ which already exists parallel to $(111)_\gamma$ across the original $\gamma - \alpha$ interface. Hence on transformation $\gamma \rightarrow \alpha$, $(111)_\gamma$ becomes $(101)_\alpha$ parallel to $(101)_\alpha$

in the pre-existing ferrite. This is consistent with the measured d spacings.

It is known that strong particles that do not have good atomic fit with the matrix act as sites for failure by decohesion or by encouraging the formation of intercritical micro-cracks at the weak interface between particles and matrix. Ideally, the good coherency at the α/martensite interface revealed by lattice imaging will prevent such decohesive interface failure during deformation, and thus enable the full toughness of the ferrite to be realized. The high resolution electron micrograph not only provides striking information on the atomic arrangement near the interface, but also allows the determination of carbon concentration in the martensite particles. Any attempt to determine the carbon concentration from the equilibrium phase diagram will be inaccurate since the two phase annealing for 20 minutes is a non-equilibrium reaction. Analytical measurements involving x-ray and electron probe techniques become extremely difficult for the submicron martensite particles (e.g., Fig. 3). Lattice fringe imaging, however, is a powerful technique in analyzing extremely localized chemical composition.

Tensile Properties

The room temperature tensile test data of the as-quenched DFM steels are plotted in Figs. 6 and 7. Fig. 6 shows the variation of yield and tensile strengths of the steels as a function of martensite volume fraction. The composite strength obeys the rule of two phase mixtures in the range of $15 \sim 80$ pct martensite, irrespective of the composition and morphology. The variation of uniform and total elongation

with respect to pct martensite are plotted in Fig. 7, which demonstrates the validity of the two phase mixture rule for elongation in the range of 10∼80% martensite. From these plots, it is clear that the 2% Si DFM steels exhibit the best combinations of strength and elongation over a wide range of pct martensite. The 0.2 pct offset yield and ultimate strengths of the duplex 2% Si steel as a function of total elongation are shown in Fig. 8, compared with some selected commercial HSLA steels including Van 80.

The attractive features of the 2% Si DFM steel are perhaps better illustrated in the characteristic stress-strain behavior (Fig. 9). The relatively low yield strength coupled with extremely high rate of work hardening in the early stage of plastic deformation of the 2% Si DFM alloys 4S1 (20% MS), 4S2 (40% MS), 4S3 (60% MS) results in high tensile/yield strength ratio and good elongation to necking, as is shown in Fig. 9. Also shown in Fig. 9 for comparison are the engineering stress-engineering strain curves for a fully martensitic structure (4A) and a commercial HSLA steel, Van 80.[16]

In the early stage of plastic deformation of the composite, the strong phase particles (martensite) do not deform with the soft phase matrix (ferrite). Mobile dislocations are impeded by the particles. The dislocation density increases rapidly as further deformation proceeds, resulting in an increase in effective size of the particles. In this way, stresses are built up, in and around the particles. The resultant stress-strain features include early and fairly extreme work hardening rates which do suppress mechanical instabilities. As a consequence, the transition from elastic to plastic deformation is smooth without

showing yield point phenomena that have been observed in a number of metals and alloys both in the single and polycrystalline state, e.g., note the yield point elongation in the load-elongation curve for Van 80. This mode of behavior continues until the yield stress of the martensite particle is reached at about 3% deformation. Here dislocations will start to cut through the semi-coherent martensite particles on the slip systems that are common to ferrite and martensite. As deformation proceeds the load required for further deformation increases. However, after the onset of large scale yielding the work hardening rate of the DFM alloys decreases and becomes virtually equal to that of Van 80, regardless of the martensite volume fraction.

The gradual equalization of work hardening rates at high strains is in agreement with calculations using finite element method,[17] which indicated that when the hard phase (martensite or carbide) yields, the work hardening rate of the composite becomes equal to that of ferrite but at a higher flow stress level.

Influence of Ferrite Purity and Martensite Strength:

It is important to understand how the properties of a DFM steel can be affected as those of the constituent phases are changed. Tempering experiments on the 2% Si DFM steel (containing $\sim$30% martensite) have been conducted to consider the case where the ferrite properties are varied while the martensite properties are kept constant.

Tempering at 200^{o}C for 1 hr did not cause any appreciable change in the morphology and mechanical properties of the martensite phase in the DFM steel. This was confirmed by transmission electron microscopy and isolated experiments measuring the mechanical properties of 100%

martensite structure before and after 200°C tempering. However, the ferrite regions which were free from any detectable precipitation in the as-quenched condition are now associated with carbide precipitation, as is seen in Fig. 10. The coarse carbides, ~170 Å wide and ~1500 Å long, were identified as cementite. The other areas in the ferrite where these coarse carbides were not present showed finely dispersed precipitation on dislocation networks, at the nodes of intersecting dislocations and at subboundaries (Fig. 11). Such a morphological change in the ferrite can be correlated with the significant increase in the elongation of the tempered DFM steel without appreciable loss in strength, as shown in Table 2. Upon tempering, the supersaturated carbon atoms in the ferrite matrix of the as-quenched DFM steel are depleted from the solution to improve ductility of the ferrite, thereby giving rise to the sharp increase in the total elongation of the DFM steel.

Now consider the case where the strength of martensite is varied while maintaining the other metallurgical variables constant. For this purpose, 1010 and 1020 steels were duplex treated to yield identical morphology of DFM structures, the only difference being the carbon concentration (higher in DFM 1020) in the martensite at a given volume pct. The results are shown in Fig. 12, where σ_y, σ_{UTS}, and uniform elongation are not significantly affected but total elongation was decreased as the martensite strength decreased. This result is consistent with the design principles described previously. The above considerations indicate that the ferrite matrix must be highly ductile and martensite

constituent strong and tough to achieve the best balance of strength and ductility of the composite at a given pct martensite.

CONCLUSIONS

1. Design principles for improved mechanical properties of DFM steels have been suggested in order to obtain desirable microstructural characteristic which in turn result in desirable mechanical properties.

2. An alloy, of composition Fe/2% Si/0.1% C, has been selected according to the design principles.

3. The 2% Si DFM steel showed high strength and good formability, e.g., $\sigma_y \sim 70$ Ksi, $\sigma_{UTS} \sim 112$ Ksi, uniform elongation $\sim 15\%$, and total elongation $\sim 25\%$ at about 40% martensite. These properties are superior to a series of Cr and Mn containing DFM steels, and to some commercial HSLA steels including Van 80.

4. Over the range of $15 \sim 80\%$ martensite, the rule for two phase mixtures appears to hold as a fairly good approximation of the tensile behavior of the duplex systems.

5. Slight improvements in the ductility of ferrite appear to cause a significant increase in the elongation ductility of DFM structures.

6. The total elongation of DFM structures is sensitive to the carbon content in the martensite phase whereas σ_y, σ_{UTS}, and uniform elongation are relatively insensitive.

7. Lattice fringe imaging of the α/martensite interface revealed that (110) fringes were continuous across the interface, indicating coherency is maintained.

ACKNOWLEDGEMENT

We would like to thank Dr. Asada and Daido Steel Company for supplying the experimental alloys used in this research. Appreciation is also extended to M. J. Young for providing some experimental data.

This work was done with support from the U.S. Department of Energy through the Materials and Molecular Research Division of Lawrence Berkeley Laboratory, University of California, Berkeley.

REFERENCES

1. K. Nakaoka, K. Araki, and O. Kimpara, Sosei to Kako, 17, No. 190, 875 (1976).
2. S. Hayami and T. Furukawa, Micro Alloying 75, Symposium on High Strength, Low-Alloy Steels, Products and Process, p. 56, Washington, D.C., 1975.
3. M. S. Rashid, SAE Preprint 760206, Feb. 1976.
4. J. Y. Koo and G. Thomas, Mat. Sci. and Engin., 24, 187 (1976) see also. J. Y. Koo, Ph. D. Thesis, University of California, Berkeley, LBL-6657, Aug. (1977).
5. A. G. Grabe, U.S. Patent 2097878, (1937).
6. S. A. Herres and C. H. Lorig, Trans. ASM 40, 775 (1945).
7. S. Morita, et al., U.S. Patent 3288657 (1966).
8. R. L. Cairns and J. A. Charles, JISI. 205, 1044 (1967).
9. R. A. Grange, Proceedings of the 2nd Int'l Conf. on the Strength of Metals and Alloys, ASM, Pacific Grove, p. 861 (1970).
10. G. Thomas, Battelle Conf. on the Fundamental Aspects of Structural Alloy Design, Richland, Washington, (Eds. R. J. Jaffee and B. A. Wilcox) Plenum Press 1977 p. 331-361.
11. E. Piwowarsky, Hochwertiges Gußeisen, Spring-Verlag, p. 52 (1951).
12. I. L. Mogford, Met. Rev., Review 114, 12, 49 (1967).
13. J. Y. Koo and G. Thomas, Met. Trans., 8A, 525 (1977).
14. A. T. Davenport, F. G. Berry, and R. W. K. Honeycombe, Metal. Sci. J., 2, 104 (1968).
15. M. Tamino and K. Aoki, Trans. Iron Steel Inst. Japan, 8, 339 (1968).

16. R. G. Davis, Ford Research Report #SR-77-29 (1977).

17. H. Fishchmeister, J.-O. Hjalmered, B. Karlsson, G. Linden, and B. Sundstrom, The Microstructure and Design of Alloys, Proc. 3rd. Int'l Conf. on Strength of Metals and Alloys, p. 621, Inst. of Metals & Iron Steel Inst., London (1973).

Table 1. Alloy Composition (wt.%)

Alloy Number	Fe	C	Cr	Si	Mn
1010	bal.	0.10	--	--	0.5
1020	bal.	0.19	--	--	0.5
2	bal.	0.06	0.49	--	--
1	bal.	0.07	2.02	--	--
5	bal.	0.07	4.00	--	--
6	bal.	0.07	--	0.49	--
4	bal.	0.065	--	2.02	--

Table 2. Tensile Test Summary (Tempered 2% Si DFM structure*)

Specimen	Tempering Temp.(°C)	σ_y (Ksi)	σ_{UTS} (Ksi)	Unif. elong.(%)	Total elong.(%)	R.A.(%)
4S	AQ**	65	110	16	23	59
4ST1	200	59	103	17	30	70

* at 30% martensite.
** As quenched.

FIGURE CAPTIONS

Fig. 1. Phase diagrams showing the expansion of the ($\alpha+\gamma$) range when silicon is added to the Fe-C system.

Fig. 2. Optical micrograph of DFM structure developed in alloy 4 (Fe/2% Si/0.1 C).

Fig. 3. Transmission electronmicrographs showing fibrous DFM structures developed in the 2 pct Si steel. Two parallel needles are martensite phase surrounded by ferrite with a high density of dislocations.

Fig. 4. Morphology of heavy precipitation of carbides in the immediate vicinity of α/martensite boundaries. (a) and (c) Bright field, and (b) and (d) corresponding Dark field image of the carbides.

Fig. 5. Conventional bright field (a) and lattice image electron microscopy (b) of a α/martensite interface in the 2% Si DFM steel. The lattice image (b) was taken from the area encircled in (a). Martensite tetragonality creates the larger d_{101} spacing in the martensite region (M). "F"-ferrite. The arrows indicate the interface.

Fig. 6. Yield and ultimate tensile strengths as a function of martensite volume fraction for DFM steels.

Fig. 7. Uniform and total elongations as a function of martensite volume fraction for the DFM steels.

Fig. 8. Tensile properties of the duplex 2% Si steel are compared with those of commercial HSLA steels.

Fig. 9. Load-elongation (engineering stress-engineering strain) curves for the 2 pct Si DFM alloy with varying amount of martensite volume fraction (20, 40, and 60%), specimen 4A having 100% martensite, and Van 80.

Fig. 10. (a) Bright field and (b) dark field electron micrographs showing precipitation of coarse carbides in a ferrite region of the 0.5 Cr DFM steel tempered at 200°C for 1 hour. (c) SAD of (a). (d) The coarse carbides, ~170 Å wide and ~1500 Å long were identified as cementite by indexing diffraction pattern.

Fig. 11. Transmission electron micrograph of a ferrite region in the 2% Si DFM steel after 200°C tempering for 1 hour, showing finely dispersed precipitation on dislocations and at sub-boundaries. (a) Bright field image does not clearly resolve the fine scale precipitates. However, weak beam image (b) shows greatly improved resolution of the heterogeneous precipitation on dislocations and at sub-boundaries. (g, 3g) weak beam imaging condition was used ((a) inset).

Fig. 12. Strengths and elongation ductility vs. martensite fraction for DFM 1010 and 1020 steels.

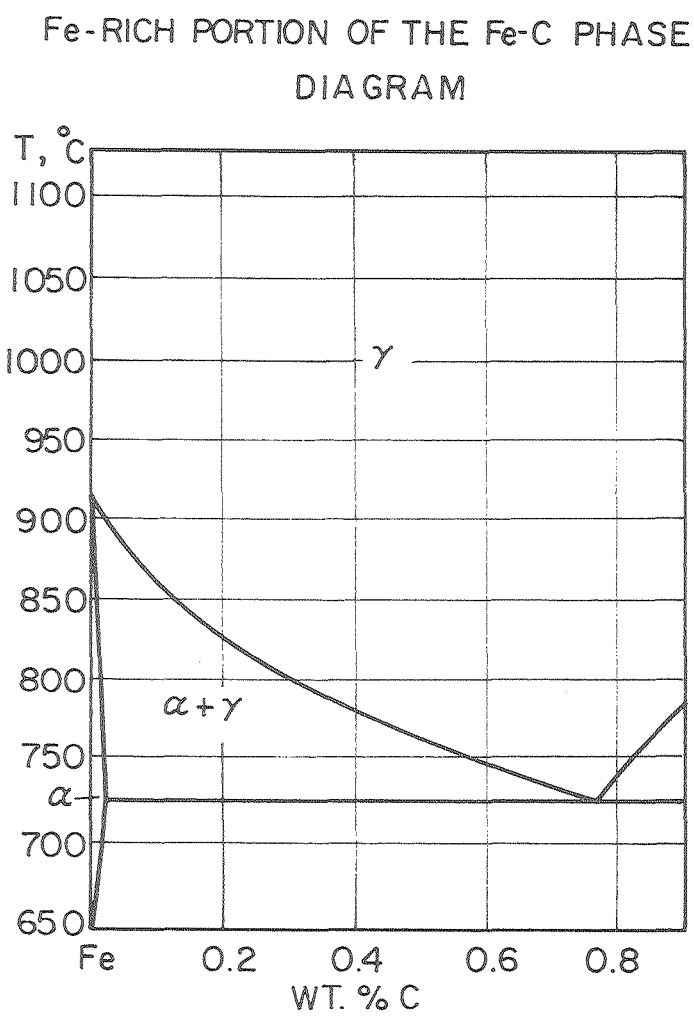

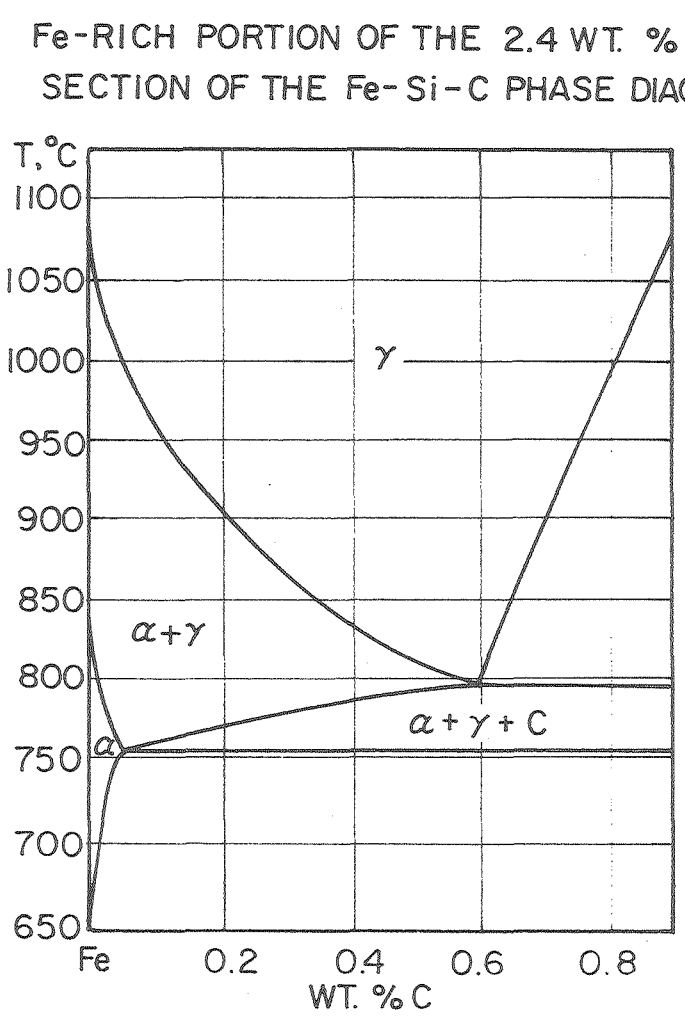

XBL 761-6344

Fig. 1.

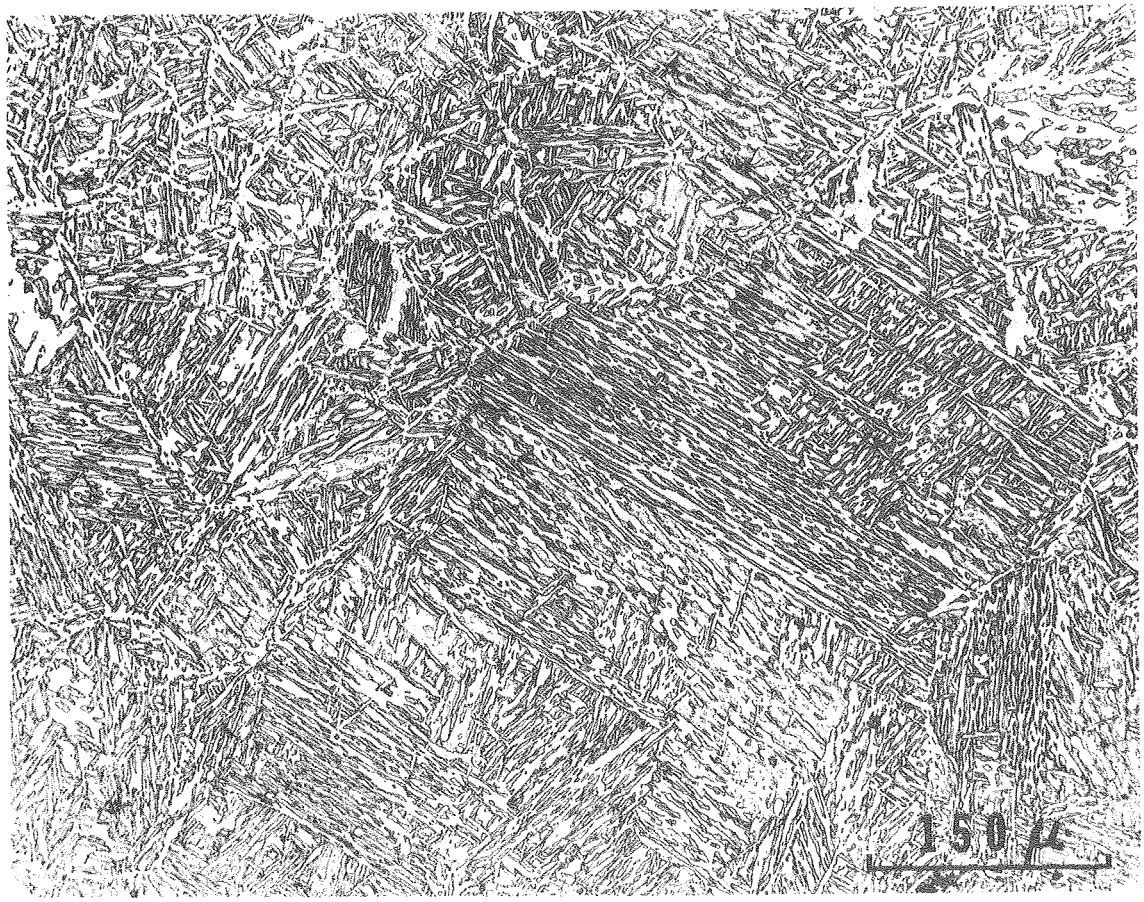

XBB 778-7551

Fig. 2.

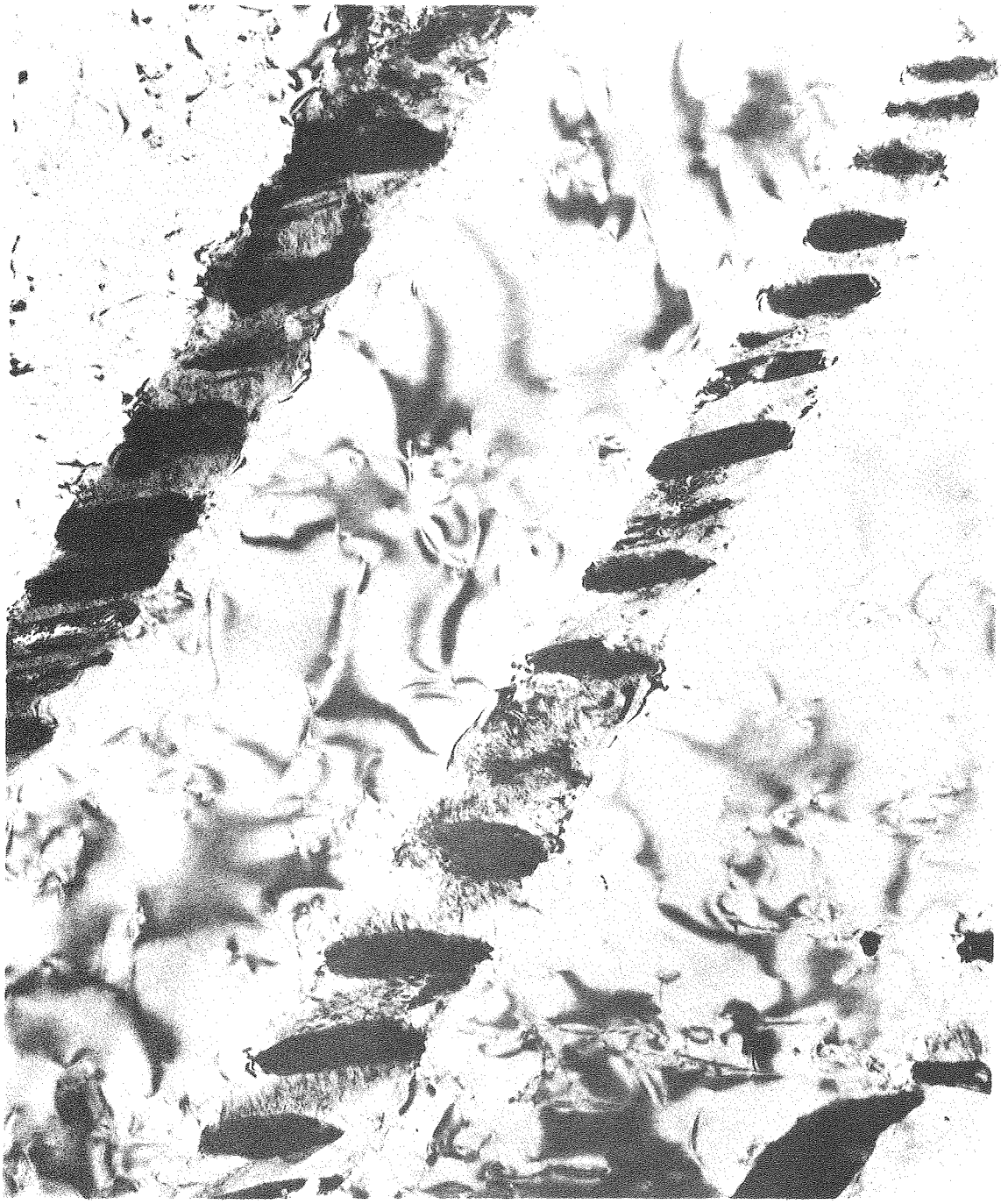

XBB 778-7555

Fig. 3.

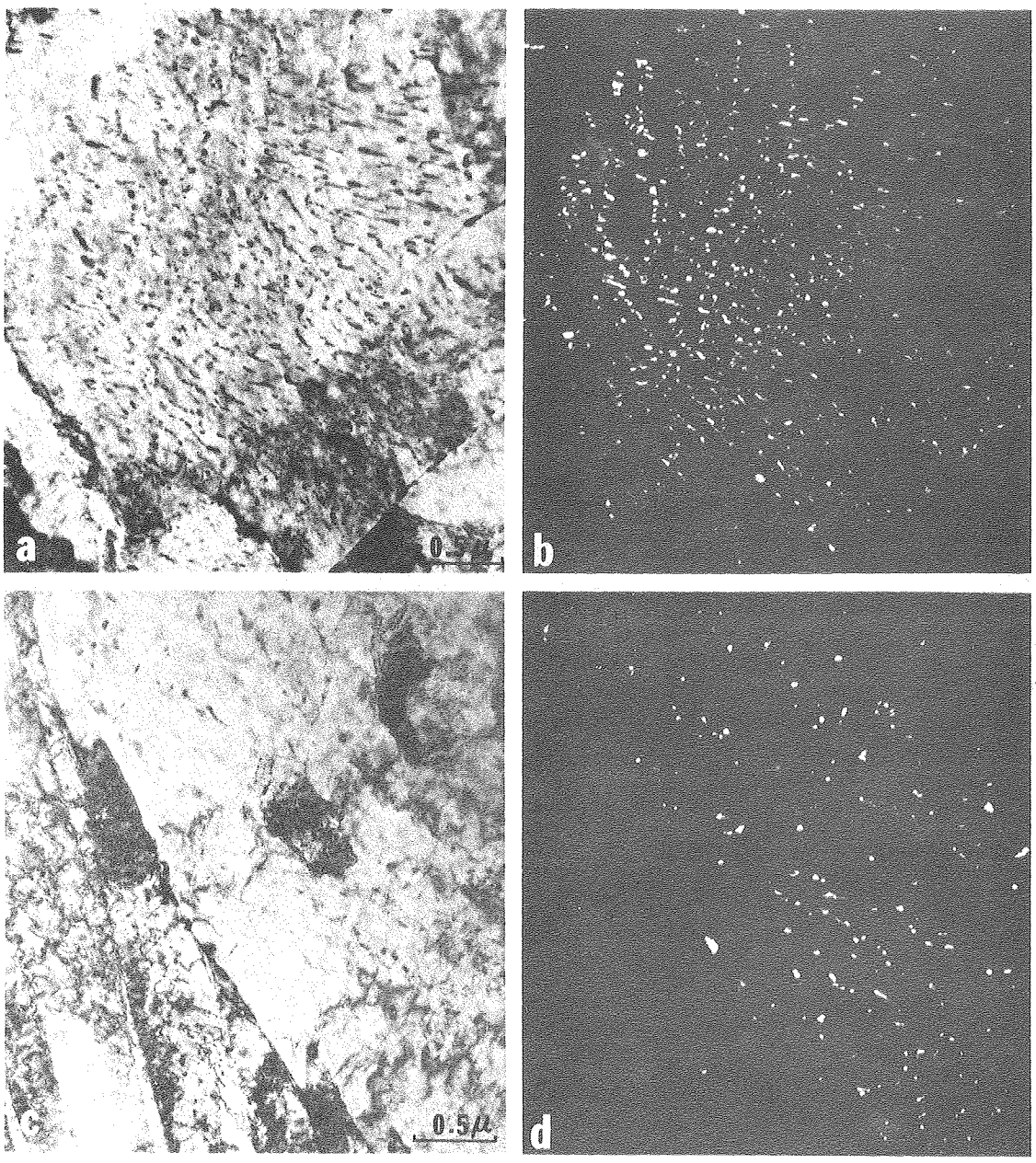

XBB 778-7556

Fig. 4.

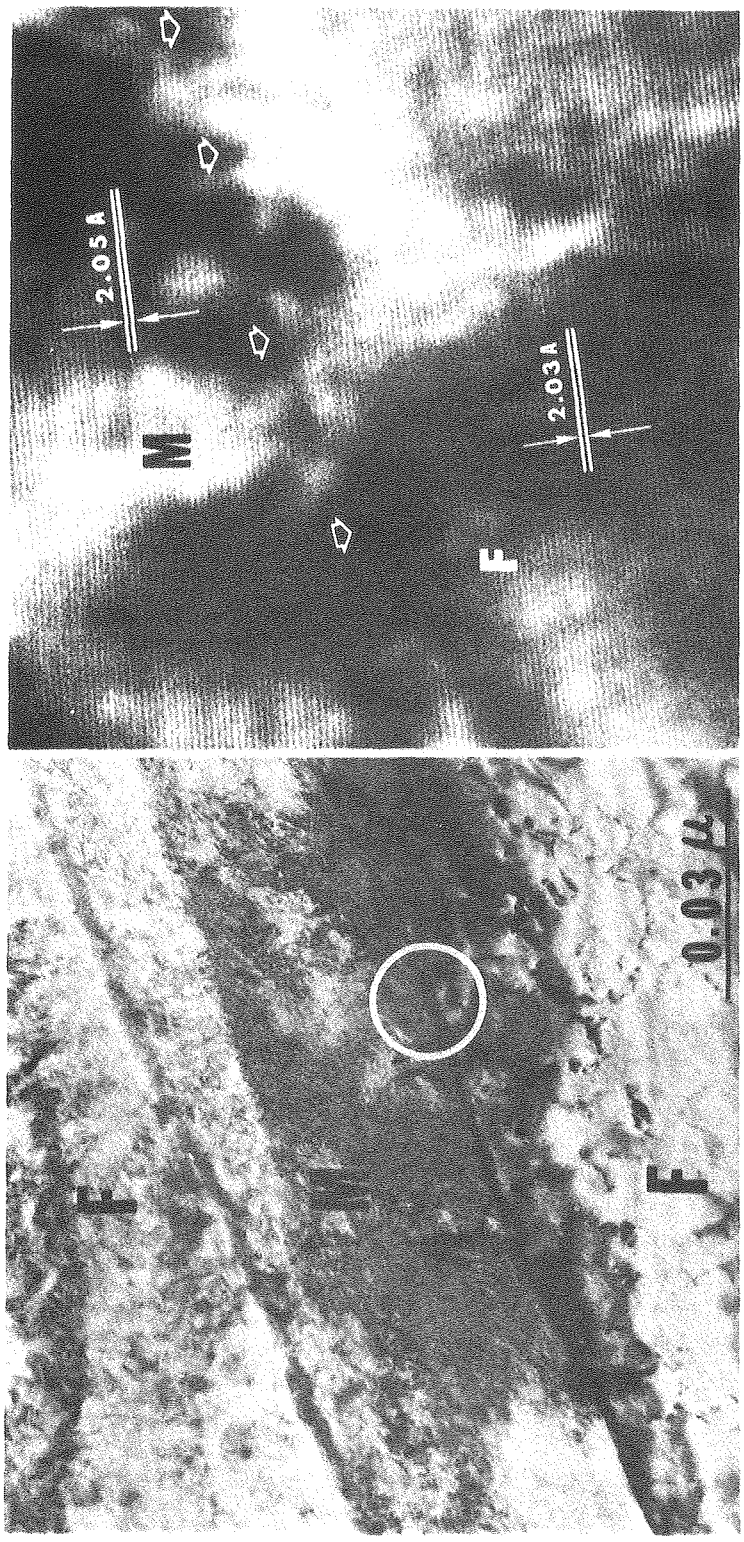

XBB 773-2297

Fig. 5.

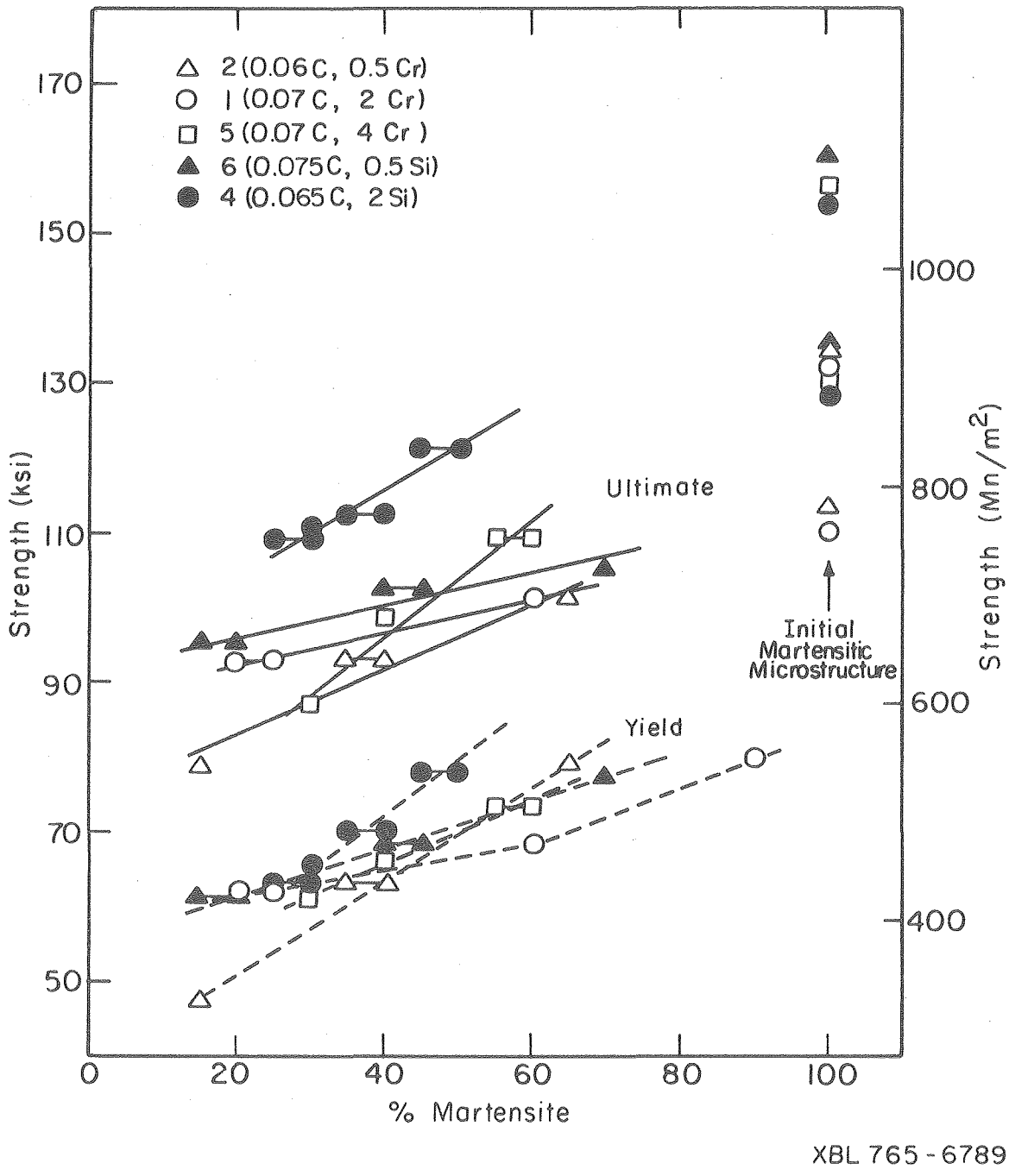
2 (0.06 C, 0.5 Cr)
1 (0.07 C, 2 Cr)
5 (0.07 C, 4 Cr)
6 (0.075 C, 0.5 Si)
4 (0.065 C, 2 Si)
Ultimate
Yield
Initial
Martensitic
Microstructure
Strength (ksi)
Strength (Mn/m²)
% Martensite
170
150
130
110
90
70
50
1000
800
600
400
0
20
40
60
80
100
XBL 765-6789

Fig. 6.

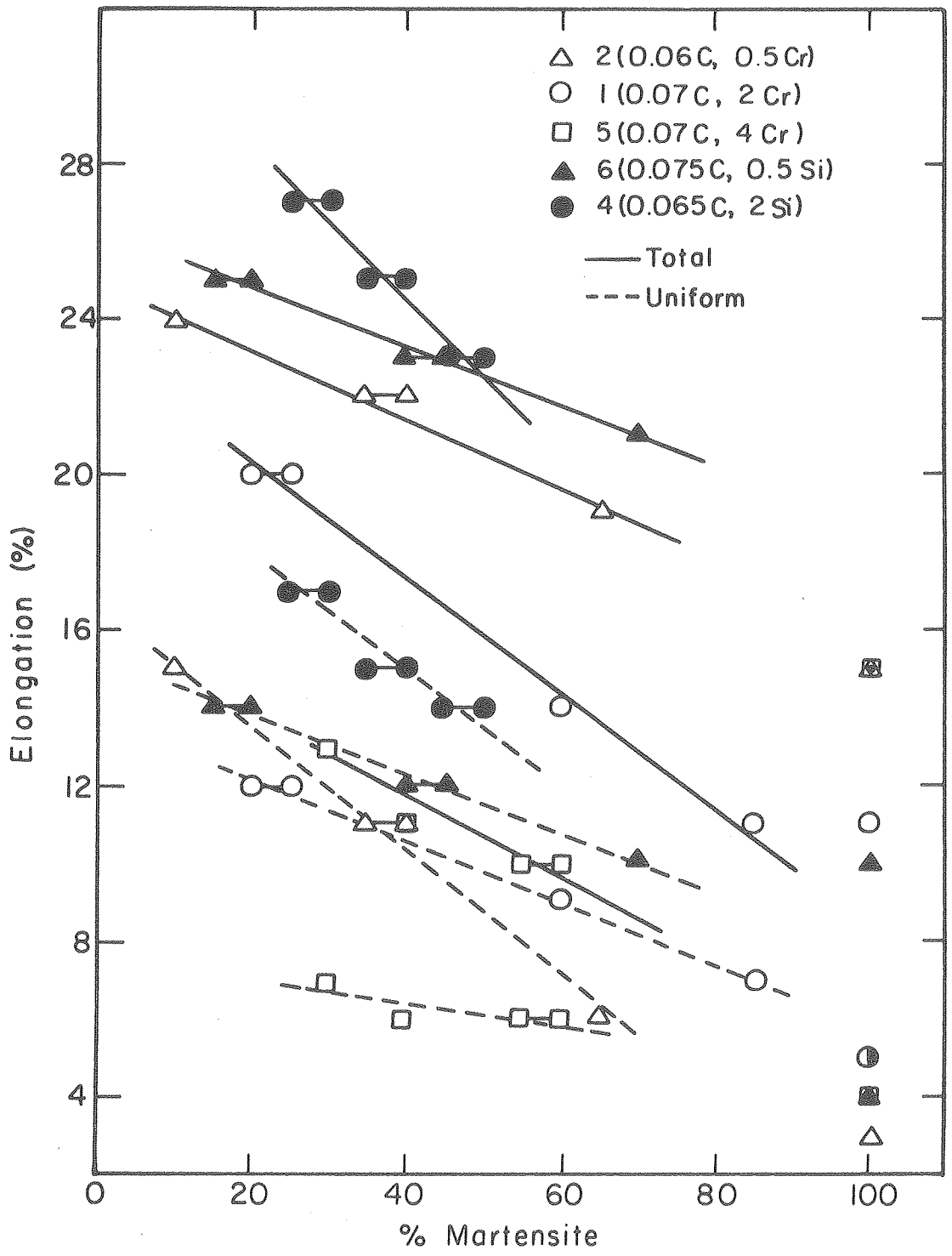

XBL 765-6788

Fig. 7.

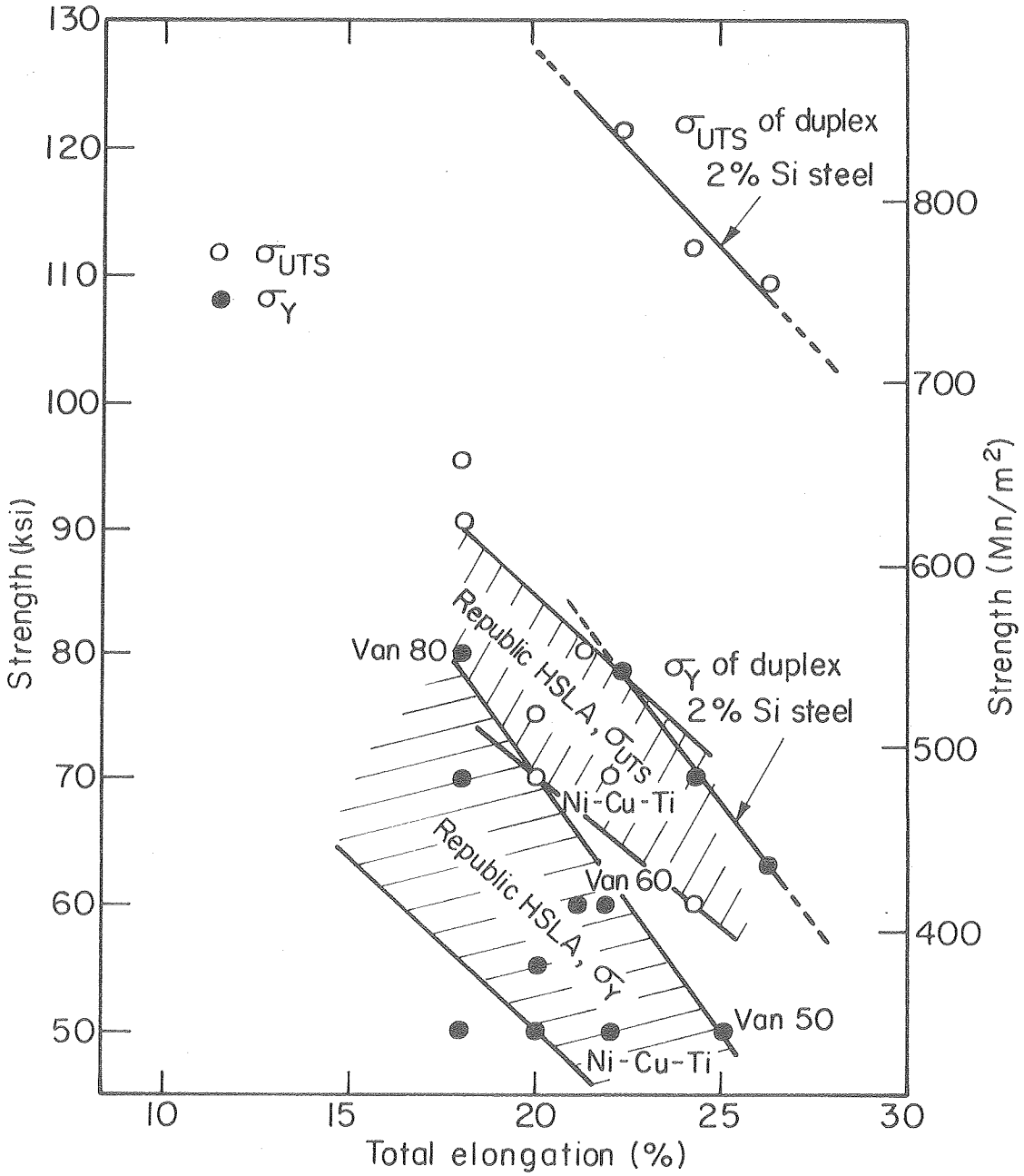

XBL766-9069A

Fig. 8.

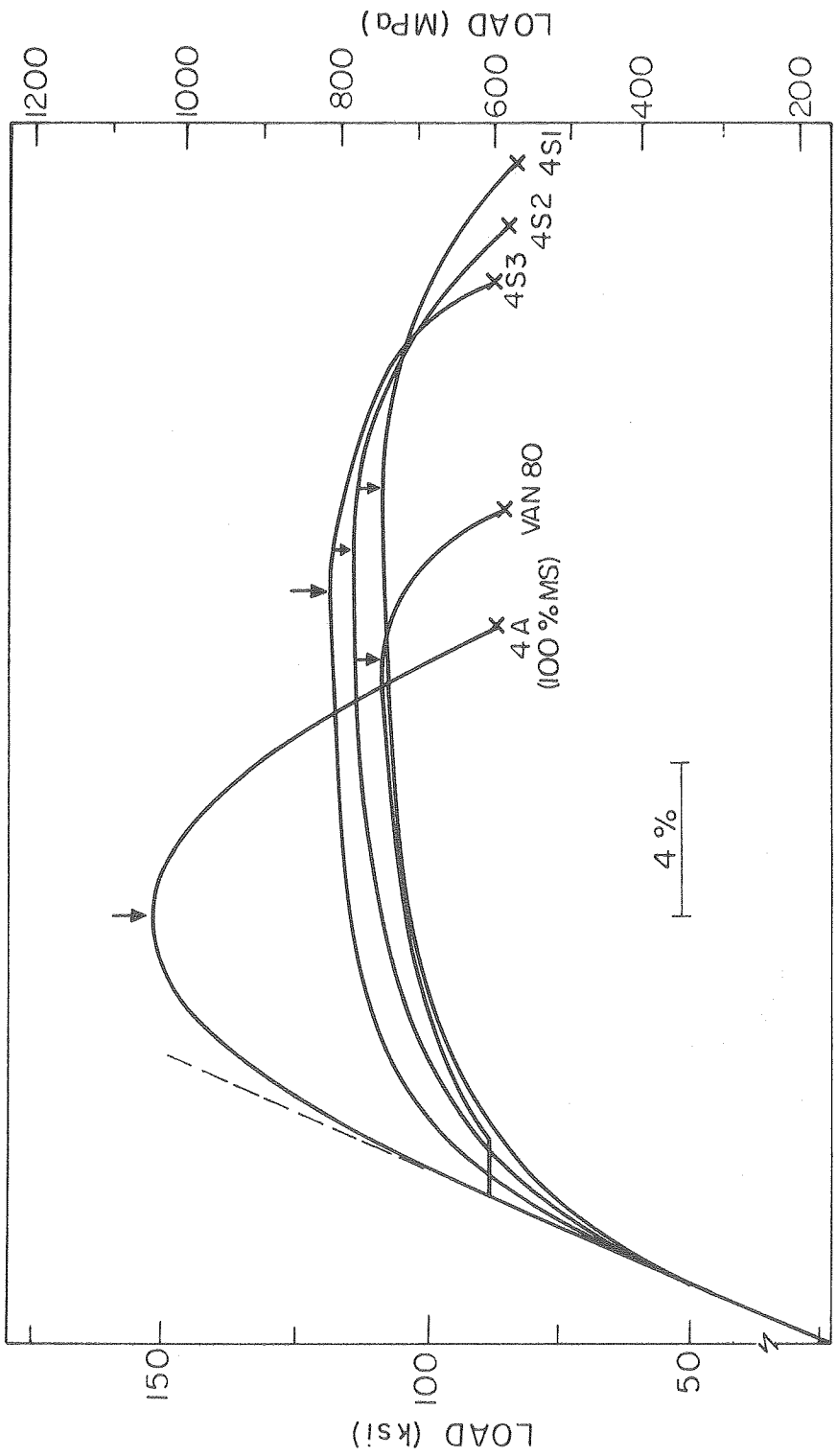

XBL 777-5865

Fig. 9.

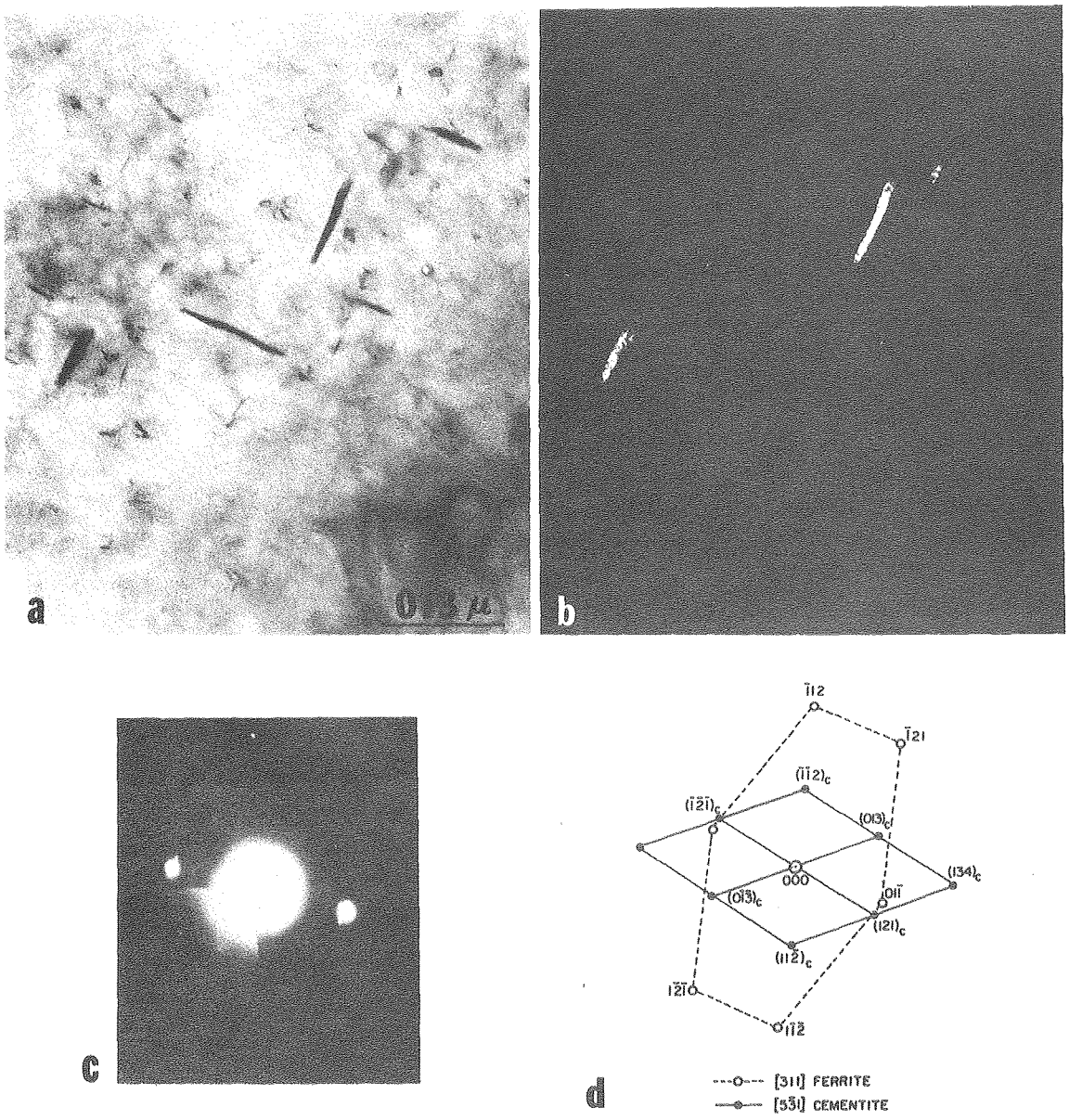

XBB 778-7540

Fig. 10.

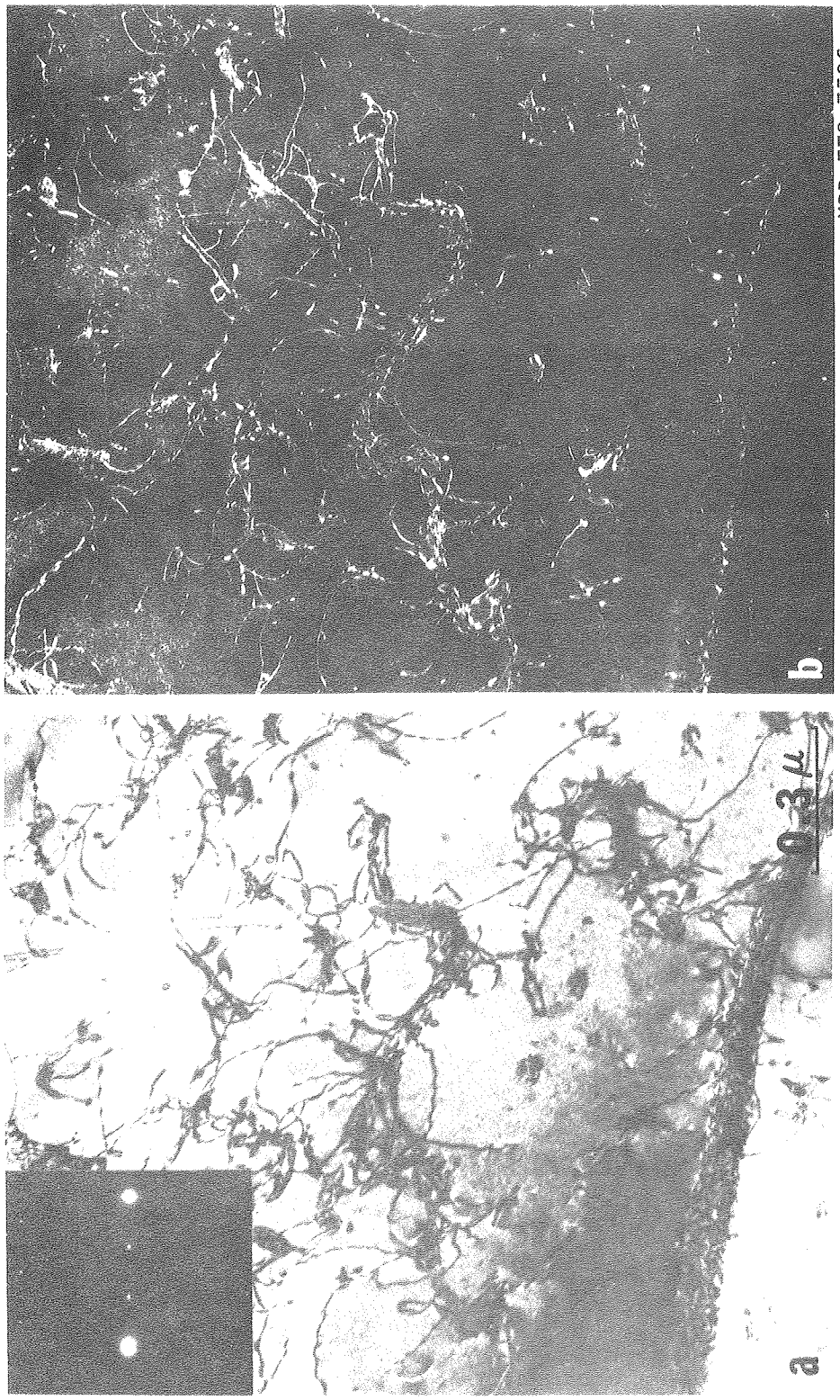

Fig. 11.

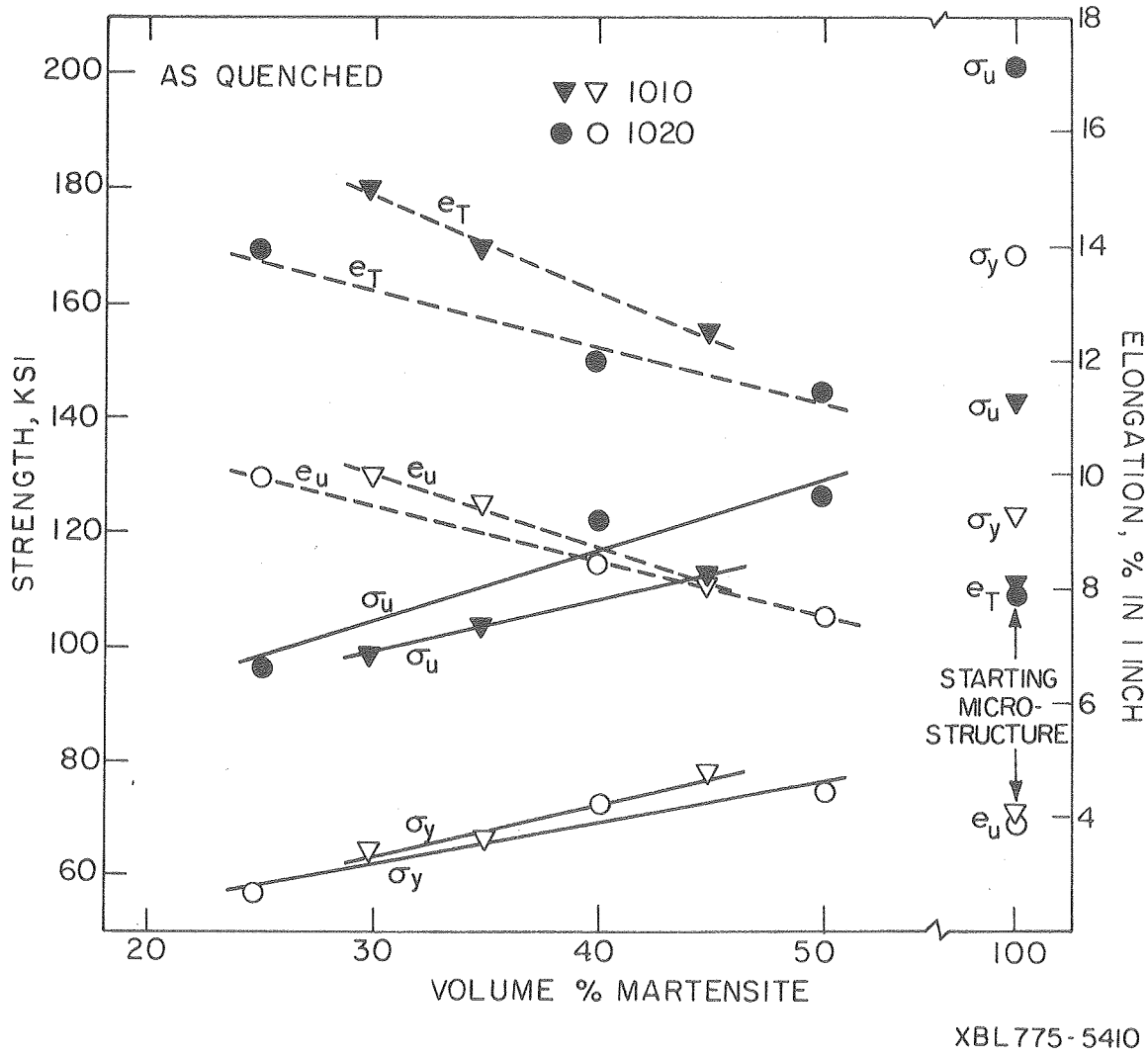
AS QUENCHED
▼▽ 1010
● ○ 1020
e_T
e_T
e_u
e_u
σ_u
σ_u
σ_y
σ_y
σ_u ●
σ_y ○
σ_u ▼
σ_y ▽
e_T
STARTING MICRO-STRUCTURE
e_u ▽ ○
STRENGTH, KSI
ELONGATION, % IN 1 INCH
VOLUME % MARTENSITE
200
180
160
140
120
100
80
60
18
16
14
12
10
8
6
4
20
30
40
50
100
XBL 775-5410

Fig. 12.

This report was done with support from the United States Energy Research and Development Administration. Any conclusions or opinions expressed in this report represent solely those of the author(s) and not necessarily those of The Regents of the University of California, the Lawrence Berkeley Laboratory or the United States Energy Research and Development Administration.